Journal of Physics: Conference Series

PAPER • OPEN ACCESS

# Comparison of OpenFOAM and EllipSys3D actuator line methods with (NEW) MEXICO results

To cite this article: J Nathan *et al* 2017 *J. Phys.: Conf. Ser.* **854** 012033

# Comparison of OpenFOAM and EllipSys3D actuator line methods with (NEW) MEXICO results

**J Nathan[1], A R Meyer Forsting[2], N Troldborg[2] and C Masson[1]**

[1]ÉTS Montral, Mechanical Engineering, Montréal H3C 1K3, Canada
[2]Technical University of Denmark, Department of Wind Energy, 4000 Roskilde, Denmark

E-mail: `joern.nathan.1@ens.etsmtl.ca`

**Abstract.** The Actuator Line Method exists for more than a decade and has become a well established choice for simulating wind rotors in computational fluid dynamics. Numerous implementations exist and are used in the wind energy research community. These codes were verified by experimental data such as the MEXICO experiment. Often the verification against other codes were made on a very broad scale. Therefore this study attempts first a validation by comparing two different implementations, namely an adapted version of SOWFA/OpenFOAM and EllipSys3D and also a verification by comparing against experimental results from the MEXICO and NEW MEXICO experiments.

## 1. Introduction

In order to circumvent the modeling of the boundary layers attached to the wind rotor blades by representing their full geometry numerically, the Actuator Line Method[1] (ALM) has become a well established alternative for more than a decade. Numerous implementations exist and are used in the wind energy research community. Often those codes were compared to experimental results such as the MEXICO experiment, which is a wind tunnel experiment with a three-bladed rotor (with a radius of $R = 4.5\,m$) conducted at the German-Dutch wind tunnels (DNW). By placing pressure sensors on the blades and using particle image velocimetry (PIV) pertinent information about the near-wake could be obtained. After some amelioration of the setup a second round of the experiment was conducted, called NEW MEXICO. For more technical details see [2] and [3].

This work picks two of the most widely used implementatons, namely EllipSys3D[4] and the SOWFA[1] project[5] in OpenFOAM. Despite the fact that some adaptions have been made to the original SOWFA code by the authors, it will be referenced as SOWFA througout the article. This work tries to presents the ability to well reproduce near wake phenomena without modeling the boundary layer on the blades and at the same time show the models limitations due to its underlying assumptions.

First there will be brief comparison of similarities and differences between the two frameworks in section 2 alongside with a description of the numerical setup. Then there will be a discussion of the results by comparing the two numerical methods against each other and against the experimental data from the MEXICO and NEW MEXICO experiment in section 3. The

[1] This implementation is part of SOWFA (Simulator fOr Wind Farm Applications) by National Renewable Energy Laboratory.

examined cases include the cases for the reference velocities $U_\infty = \{10, 15, 24\}\, m/s$ and for the comparison with the experiment the PIV sheets and force measurements are used. Finally some concluding remarks will be given in section 4.

## 2. Numerical method

### *2.1. Numerical framework*

Both implementations have been done within a CFD framework based on the control volume method with variables located at cell center and a Rhie-Chow[6] like correction. For a more in-depth description of the underlying CFD methods see [7] and [8].

In both cases the rotor is modeled by a force inserted as a momentum sink in the Navier-Stokes equations and distributed by a Gaussian distribution in order to avoid non-physical spikes in the velocity field around the affected cells. While SOWFA specifies a cut-off length for the 3D Gaussian curve in order to recover approximately 99.9% when integrated, the cut-off length of EllipSys3D is significantly larger to contain an even higher percentage. These two different cut-off lengths do not seem to have a significant impact on the simulation results.

Velocities are sampled in a very similar manner. While EllipSys3D uses explicitly trilinear interpolation to obtain the sampled velocity at the actuator point, SOWFA relies on correcting the cell center value by the velocity gradient. In the present case this gradient is obtained by linear interpolation and hence both sampling methods behave the same way.

While there are efforts to modify the orignal 2D airfoil coefficient data such as[9], the present work wants to use the ALM as an a priori tool. Hence the ALM is relying on the original airfoil data obtained from wind tunnel experiments of an infinite wing. As the centrifugal forces of the rotating blades keep the boundary layer attached longer than on a non-rotating wing [10], the angle of attack (AOA) for the maximum $c_L$ is expected to be shifted towards higher values. Therefore it is expected that this ALM will lead to discrepancies between simulation and experiment for AOAs beyond the angle where stalling occurs in the airfoil data.

A tip correction is applied on the calculated forces. Without the tip correction, the forces where much higher than predicted by experiment. This is most probably due to the under-resolved tip vortex resulting in a weaker down-wash than in the experiment. By conducting the same simulation at different resolutions around the rotor, a higher induction in the tip region can be noticed. In order to compensate for this effect a Glauert tip correction is applied. This resulted also in a better agreement with the experimental data.

### *2.2. Numerical setup*

The computational domain is cubic with an edge length of $20R$ with $R$ as the rotor radius and the rotor positioned at the domain center. In both cases the cells in the vicinity of the rotor are cubic with the size $\Delta x = R/32$ and are stretched towards the domain boundaries in the case of EllipSys3D. Within SOWFA several refinement zones are applied each time halfing the cell edge length. Therefore the mesh of EllipSys3D consists of 7.1e6 cells while the mesh of the SOWFA case consists of $1.9e6$ cells.

For both cases the velocity boundary condition are given by a uniform inflow velocity of $\mathbf{U} = (U_\infty,\, 0,\, 0)$ and a zero gradient at the outlet. The lateral boundaries are set as symmetric.

As both simulations are Large Eddy Simulations, the subgrid-scale models are the dynamic Lagrangian method based on[11] for the SOWFA case and a DES model using a limiter to switch between $k - \omega$ SST and LES[12] for the EllipSys3D case. But as there is no inflow turbulence and the helical vortex structure does not break up within the examined region, not a lot of turbulence modeling has to be done. When comparing to a very coarse DNS by deactivating the sub-grid scale model, no significant difference is found.

The SOWFA case uses a discretisation scheme for the convection term that blends 75% of second order central differencing with 25% linear upwind differencing, which is a second

IOP Conf. Series: Journal of Physics: Conf. Series **854** (2017) 012033 doi:10.1088/1742-6596/854/1/012033

order upwinding scheme, where the face value is corrected by the gradient in the upwind cell. EllipSys3D applies QUICK in RANS regions and central differencing of fourth order in LES regions using the same limiter as for DES model.

For parametrisation of the ALM the Gaussian distribution parameter is set at $\epsilon = 2\Delta x$ and 40 actuator points are used to represent one blade.

## 3. Results

The first interesting observation is the similarity in sampled velocities and AOAs as shown in figure 1 and figure 2. The directions in figure 2 are based on a local coordinate system on the blade. Despite the existence of steep velocity gradients due to the bound vorticity both frameworks obtain very similar values. This even holds for the relative small value of the

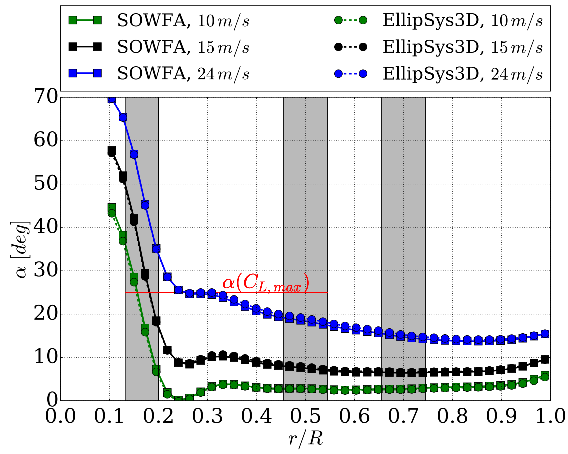


**Figure 1.** Angle of attack $\alpha$ for each actuator point along the blade. The grey zones represent transition between different airfoil types and the red line (—) the AOA for which the inbound airfoil data indicates stalling.

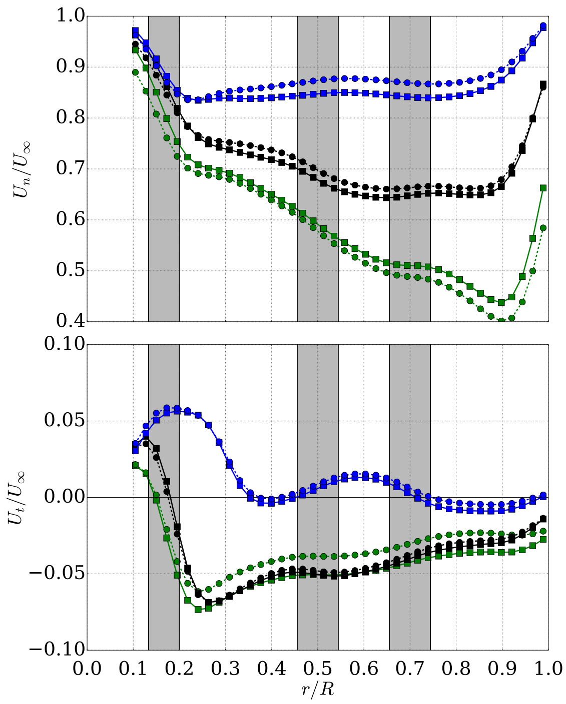


**Figure 2.** Normalized normal velocity and tangential velocity component $U_n/U_\infty$ and $U_t/U_\infty$ for each actuator point along the blade. The grey zones represent transition between different airfoil types. (see legend in figure 1)

tangential velocity component.

When looking at the AOAs in figure 1 it can be seen that for the radial position $r/R < 0.3$ at $U_\infty = 24\,m/s$ it exceeds the angle after which stalling occurs according to the 2D airfoil data. For the other cases and airfoil sections the AOA always remains below the critical angle. Hence the ALM with the unaltered airfoil data breaks for the aforementioned case and the calculated forces will not match the ones obtained experimentally. In figure 3 the body forces associated with rotating blades can be seen. Again the directions are based on a local coordinate system on the blade. For $U_\infty = 10\,m/s$ and $15\,m/s$ exists a very good agreement, while the forces are not correctly evaluated for the high velocity case. A sudden drop in both forces can be seen. This is stemming from the fact that beyond a certain AOA no experimental data is available

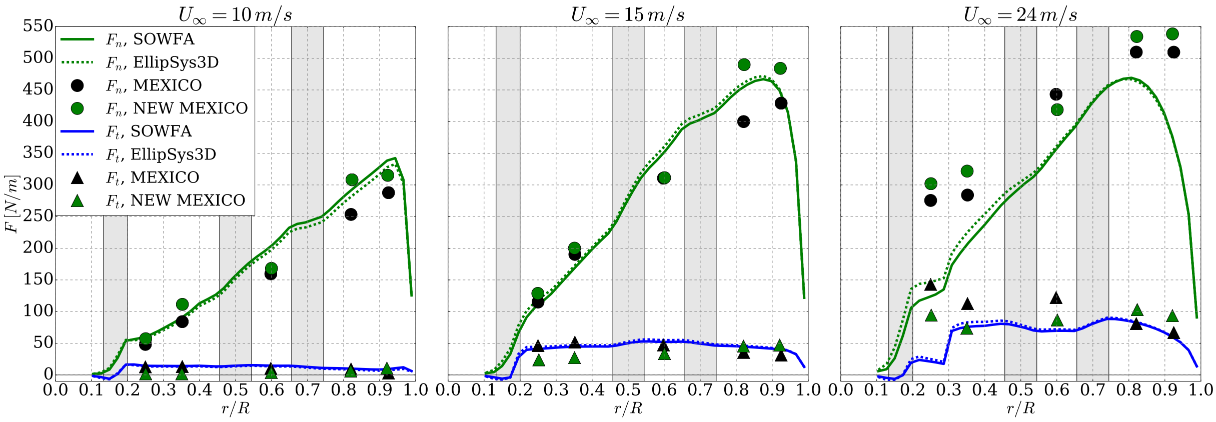


**Figure 3.** Comparion between the evaluated normal and tangential blade forces $F_n$ and $F_t$ by SOWFA and EllipSys3D against the experimental results of MEXICO and NEW MEXICO over the radial position.

and the void was filled by using the flat plate assumption. Therefore the airfoil data has a sharp drop in the lift coefficient at this point. Another interesting observation is that the forces for the MEXICO experiment are lower than for the NEW MEXICO experiment. This is probably due to the fact that the experiments were conducted with a slightly lower inlet velocity. Again the SOWFA and the EllipSys3D case are very similar even in the case where the models break down.

Due to the slight difference in the blade forces both frameworks produce a relatively similar flow field as shown in figure 4. In the following visualisations the flow field data is based on the domain coordinate system with $x$ in flow direction, $r$ parallel to the rotor plane and lying in the PIV sheet and $t$ as the tangential direction normal to the PIV sheet. The blade position is expressed by the angle $\Psi$ whereas $\Psi = 0$ means that the first blade is pointing upwards. It can be seen that neither SOWFA nor EllipSys3D can simulate distinct vortices shed in the case of turbulent wake state ($U_\infty = 10\,m/s$), but instead a continuous vortex is shed from the rotor. This is due to the rather coarse resolution of $R/32$. With higher inlet velocities a vortical structure can be noticed.

When looking at the radial profiles of the axial, normal and tangential velocity components $U_x$, $U_r$ and $U_t$ in figure 5 and figure 6, it can be seen that in general both frameworks are underestimating the velocity deficit in the ultimate rotor vicinity ($x/R = \pm 0.13$) compared to the experimental results but the overall trend is very well maintained. An exception is the high velocity case ($U_\infty = 24\,m/s$) where the models deficit becomes appearant. The high gradient of the radial velocity component in the tip region seems to be smeared out by the numerical simulation as can be seen in figure 6. This is most probably due to the numerical schemes and the mesh discretisation, which is expected to ameliorate when using a finer resolved mesh around the rotor. This would not only lead to a better resolution of the vortical structures, but due to the fixed force distribution parameter $\epsilon = 2\Delta x$ also to a more realistic distribution of the force in the tip region. The same applies to the tangential velocity component in the root region.

The axial profiles of the velocity components can be seen figure 7 and figure 8 and again both codes reproduce very similar results in the near wake further away from the rotor. While for the inbound position only data from NEW MEXICO experiments for $U_\infty = 15\,m/s$ are available, we can look at a bigger picture for the outbound position shown in figure 8. Again simulation results are very close to experimental data from the NEW MEXICO experiment, while overestimating with respect to MEXICO results due to reasons already mentioned. For

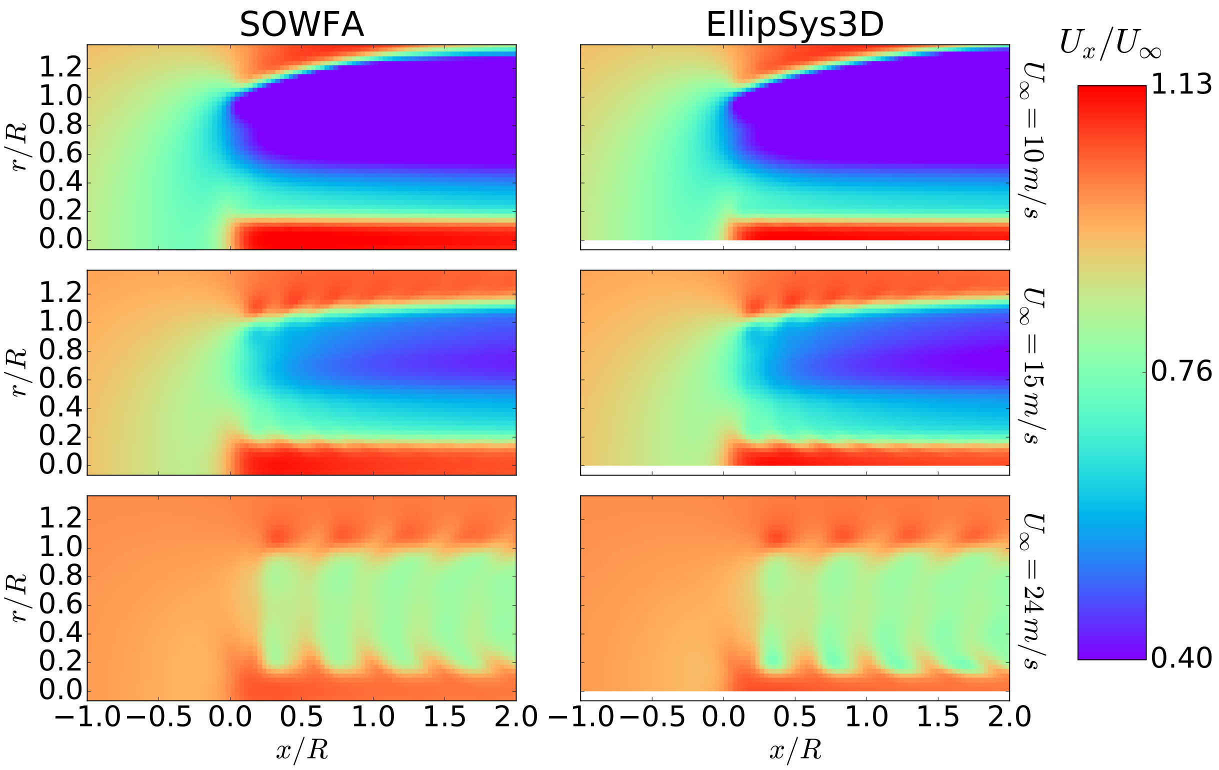


**Figure 4.** Planes of normalized axial velocity component $U_x/U_\infty$ for all three cases for SOWFA and EllipSys3D. The rotor is situated at $x/R = 0$ and the velocity field is phase averaged for the rotor position $\Psi = 0^o$.

the high velocity case ($U_\infty = 24\,m/s$) the vortex sheets shed from the blades become visible by the oscillations in the axial velocity component $U_x$.

When looking at the vortex properties as examined in [13] in figure 9 and figure 10. it can be seen that there is a good general agreement despite the coarse resolution of the grid around the rotor ($\Delta x = R/32$). In figure 9 the vortex locations were calculated based on a rotor position of $\Psi = 0^o$ while the experimental was taken for $\Psi = 30^o$, which is the moment when the blade crosses the PIV sheet. Despite the fact that the origins of the vortices might not coincide as stated in [13] and the wake deficit was lower than in the experiments, the simulations appear to represent well the vortex propagation. This can also be seen by looking at figure 9 and comparing the axial locations of the vortices compared to the experimental results. Differences between the two simulations as seen in figure 9 stem from discrete representation of the vortices. In a more refined mesh both curves are expected to be closer.

In order to evaluate the vortex strength the circulation for each vortex is calculated. For obtaining the circulation of the vortices the vorticity magnitude $\omega$ in the plane at $\Psi = 0^o$ is integrated over a square with the edge length $R_S$ weighted by the area. When looking at the evolution of vortex circulations in figure 10 it can be seen that the circulation remains almost constant througout the examined region, despite the fact that a constant integration radius $R_S$ was used in order to evaluate the total circulation $\Gamma$. In figure 10 the total circulation can be seen in dependence of the square edge size $R_S$. At around $R_S/R = 0.113$ the saddle point can be perceived. Upto this point the integration only includes vorticity due to the examined vortex. Beyond that $R_S$ also the vorticity of the neighbouring vortices is taken into account hence the steeper increase in circulation.

IOP Conf. Series: Journal of Physics: Conf. Series **854** (2017) 012033 doi:10.1088/1742-6596/854/1/012033

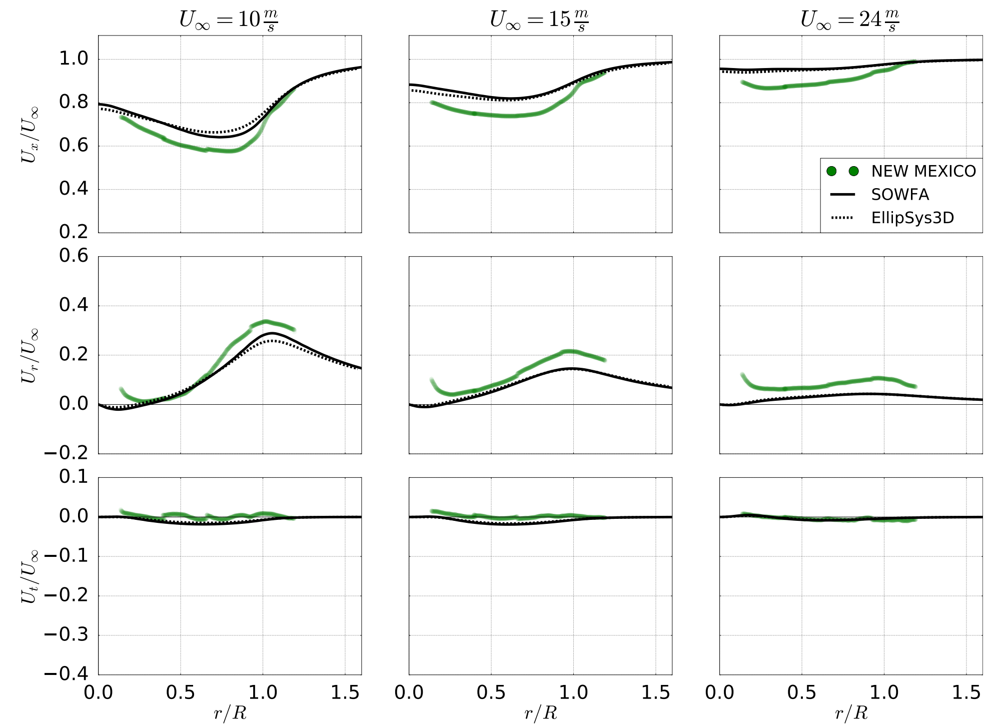


**Figure 5.** Radial profile of phase averaged ($\Psi = 0^o$) velocity components for different flow cases at upstream ($x/R = -0.13$) position.

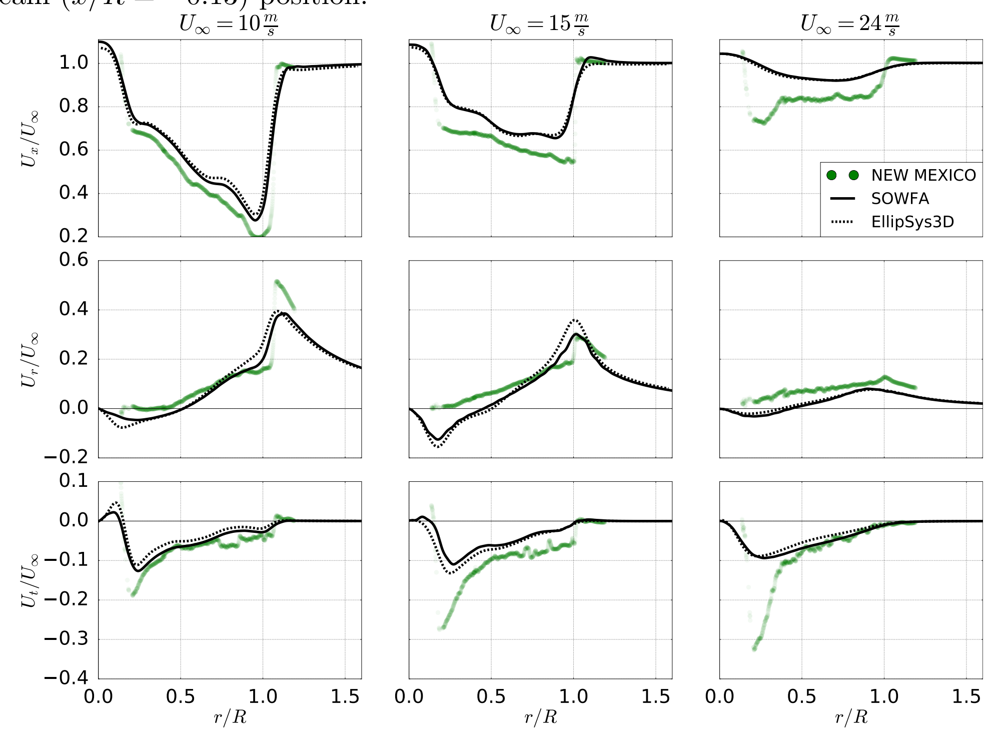


**Figure 6.** Radial profile of phase averaged ($\Psi = 0^o$) velocity components for different flow cases at downstream ($x/R = 0.13$) position.

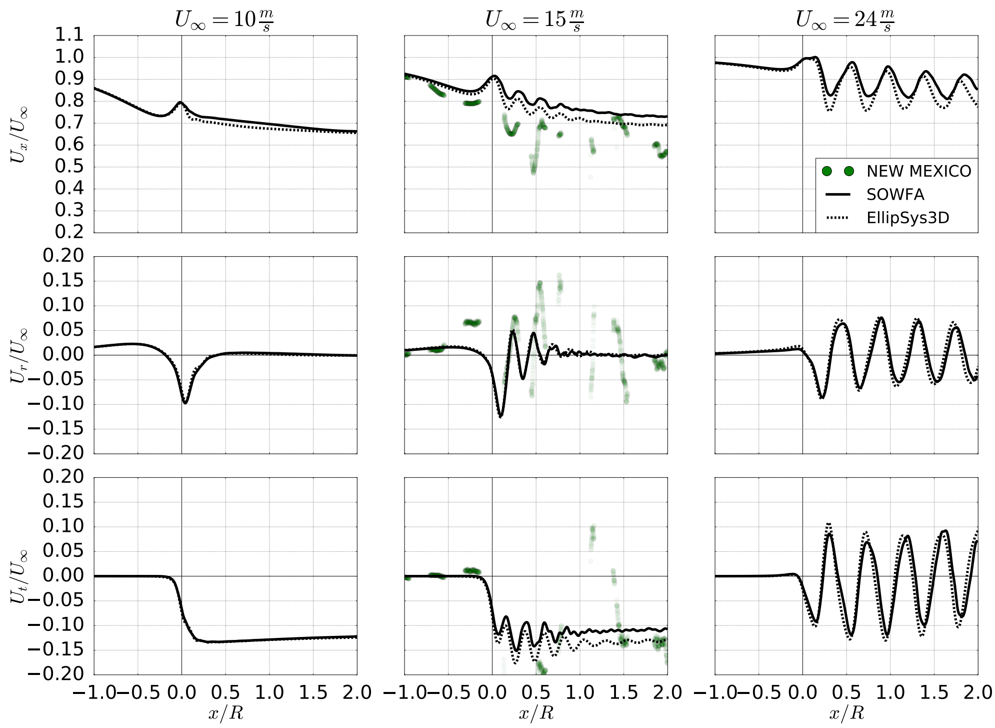


**Figure 7.** Axial profile of phase averaged ($\Psi = 0^o$) velocity components for different flow cases at inbound ($r/R = 0.22$) blade position.

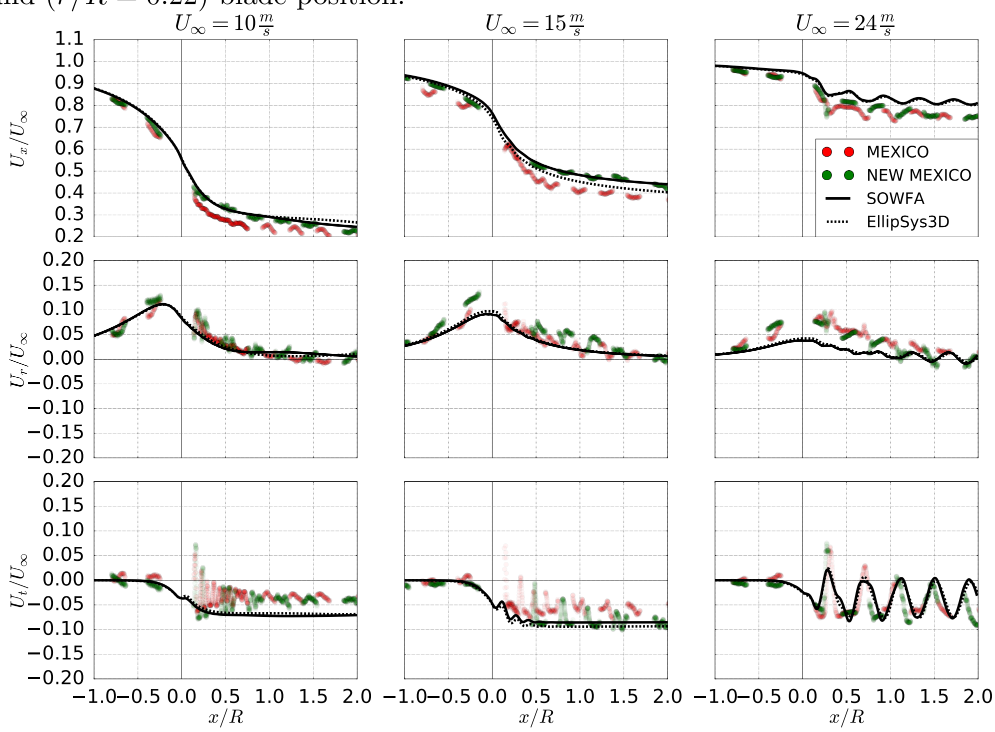


**Figure 8.** Axial profile of phase averaged ($\Psi = 0^o$) velocity components for different flow cases at outbound ($r/R = 0.67$) blade position.

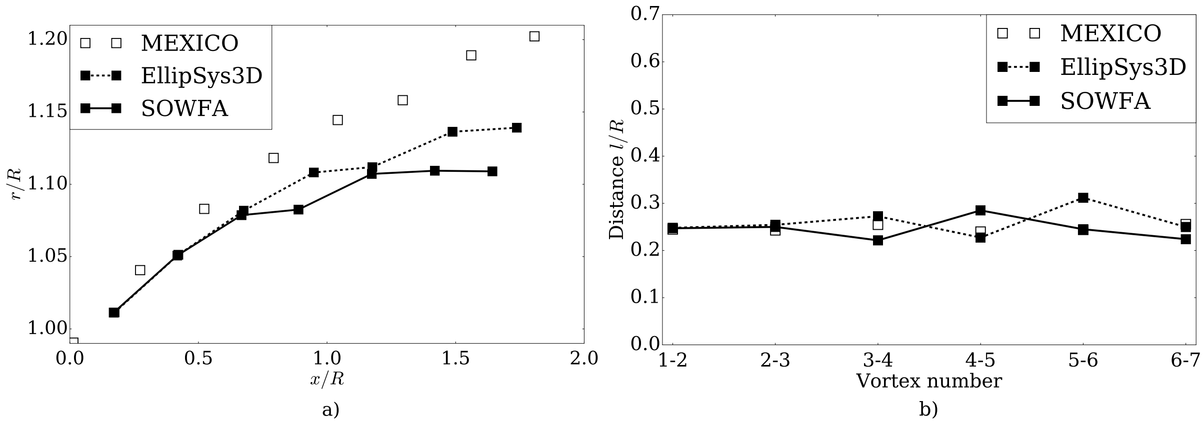


**Figure 9.** Normalized vortex locations (a) and distances (b) for $U_\infty = 15\,m/s$.

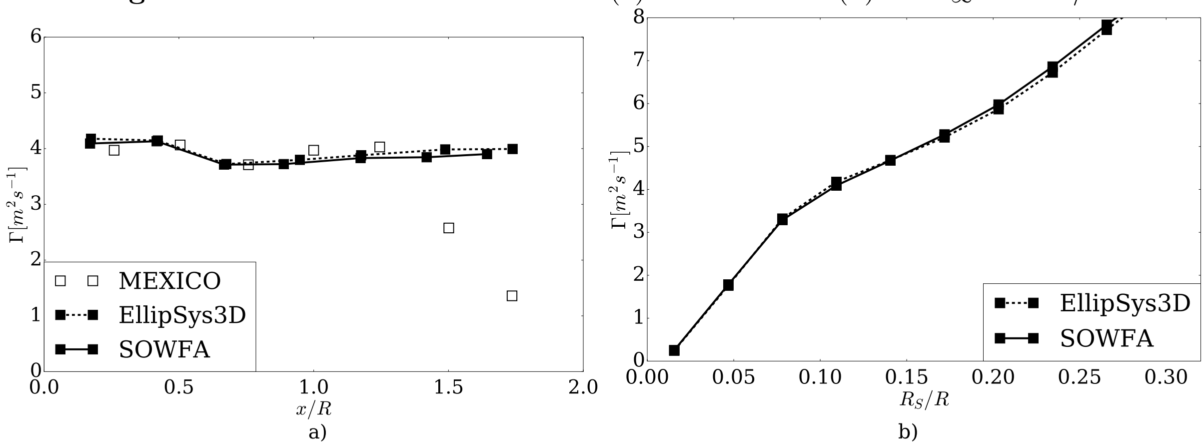


**Figure 10.** Circulation of vortices (a) and integration radius $R_S/R$ (b) for $U_\infty = 15\,m/s$.

## 4. Conclusion

The two examined frameworks, EllipSys3D and SOWFA, compare very well in the near wake of the rotor used in the MEXICO and NEW MEXICO experiment. When comparing them against experimental data it can be seen that they predict well the experimental results from the NEW MEXICO experiment while there is an overprediction compared to MEXICO results due to the inlet velocity mismatch in this experiment. Even vortex properties matched among the simulations and predicted the same trend as in the MEXICO experiment, although the resolution in the rotor vicinity might be too coarse for well resolving the helicoidal vortex structure.

Both frameworks obtain very similar velocites and AOAs, and fail at the moment where 3D effects start to dominate. As this occurs only for a very high velocity at the inbound region, it is very encouraging for using only non-altered airfoil data in the presented case.

Future work could be to conduct simulations with a finer resolved region around the rotor and also to find a suitable method for including 3D effects in order to reproduce well the results for the high velocity case. Furthermore the influence of a turbulent inflow could be examined as well.

## Acknowledgments

This work is partially supported the Canadian Research Chair on the Nordic Environment Aerodynamics of Wind Turbines, the Natural Sciences and Engineering Research Council

(NSERC) of Canada, the Innovation Fund Denmark (grant number 1305-00024B) and DTU Risø central computing facilities. Thanks for the great work done by Matthew Churchield and colleagues at National Wind Technology Center, Boulder, CO, by establishing the open source framework SOWFA. The data used have been supplied by the consortium which carried out the EU FP5 project Mexico: 'Model rotor EXperiments In COntrolled conditions'. The consortium received additional support to perform the New Mexico measurements from the EU projects ESWIRP and INNWIND.EU.

## References

[1] Sørensen, J. N. and Shen, W. Z., 2002. Numerical Modeling of Wind Turbine Wakes. *Journal of Fluids Engineering*, 124(2), pp. 393.

[2] Schepers, J. G. and Snel, H., 2007, *Model Experiments in Controlled Conditions, Final report*, Report, ECN-E-07-042, Energy Research Center of the Netherlands, ECN.

[3] Schepers, J.G., Boorsma K. et al., 2014, *Final report of IEA Task 29, Mexnext (Phase 2)*, Report, ECN-E-14-060, Energy Research Center of the Netherlands, ECN.

[4] Troldborg, N., 2008, *Actuator Line Modeling of Wind Turbine Wakes*, PhD Thesis, Technical University of Denmark, Copenhagen.

[5] Churchfield M J, Lee S, Michalakes J and Moriarty P J 2012 A numerical study of the effects of atmospheric and wake turbulence on wind turbine dynamics *Journal of Turbulence* 13

[6] Rhie, C.M. and Chow, W.L., 1983. Numerical study of the turbulent flow past an airfoil with trailing edge separation, *AIAA journal*, 21(11), pp. 1525–1532.

[7] Sørensen, N. N., 1995, *General Purpose Flow Solver Applied to Flow over Hills*, PhD thesis, Technical University of Denmark, Copenhagen.

[8] Jasak, H., 1996, *Error analysis and estimation in the Finite Volume method with applications to fluid flows*, PhD Thesis, Imperial College, University of London.

[9] Shen, W. Z., Zhu, W. J., and Sørensen, J. N., 2012, Actuator line/NavierStokes computations for the MEXICO rotor: comparison with detailed measurements, *Wind Energy*, 15(5), pp. 811–825.

[10] Vermeer, L. J., Sørensen, J. N., and Crespo, A., 2003, Wind turbine wake aerodynamics, *Progress in Aerospace Sciences*, 39(67), pp. 467–510.

[11] Meneveau, C., Lund, T. and Cabot, W., 1996, A Lagrangian dynamic subgrid-scale model of turbulence, J. Fluid Mech, vol 319, pp. 353–385.

[12] Troldborg, N., Zahle, F., Rthor, P.-E. and Sørensen, N. N., 2015, Comparison of wind turbine wake properties in non-sheared inflow predicted by different CFD rotor models, *Wind Energy*, 18(7), pp. 1239–1250.

[13] Nilsson, K., Shen, W. Z., Sørensen, J. N., Breton, S.-P., and Ivanell, S., 2015, Validation of the actuator line method using near wake measurements of the MEXICO rotor, *Wind Energy*, 18(9), pp. 499–514.